J. Astrophys. Astr. (2001) **22,** 145–154

Hard X-ray Spectrum of Mkn 421 during the Active Phase

R. K. Manchanda *Tata Institute of Fundamental Research, Colaba, Mumbai 400 005, India*
e-mail: ravi@tifr.res.in

Received 2001 July 27; accepted 2001 September 27

Abstract. Spectral measurement of Mkn 421 were made in the hard X-ray energy band of 20–200 keV using a high sensitivity, large area scintillation counter telescope on November 21, 2000 and these coincided with the onset of an active X-ray phase as seen in the ASM counting rates on board RXTE. The observed spectrum can not be fitted to a single power law similar to the PDS data of BeppoSAX. The data can be fitted both by a two component power-law function or a combination of an exponential function with a power law component at the high energies above 80 keV. We identify these components with those arising from the synchrotron self compton and the high energy power-law tail arising from the upgrading of the thermal photons due to multiple Compton scattering a la Cyg X-1. A comparison with the earlier data clearly suggests a spectral variability in the hard X-ray spectrum of the source. We propose a continuously flaring geometry for the source as the underlying mechanism for energy release.

Key words. X-rays; AGNs—BL Lac sources, massive black hole candidates, jet emission; individual—Mkn 421.

1. Introduction

Among the active galactic nuclei, blazers form a distinct class of highly luminous, radio loud and rapidly variable objects in the entire electromagnetic spectrum. The X-ray spectra of these sources extend from the soft X-ray region of < 1 keV to the TeV energy band. Mkn 421 is the brightest of the BL Lac objects in the X-ray band and the photon flux has been observed up to $> 10^2$ eV. This source was the first BL Lac object to be discovered in X-rays (Ricketts *et al* 1976) and hard X-ray spectrum up to 100 keV was first measured by Ubertini *et al* (1984). The source has been repeatedly studied in different wave band regions of radio, UV, X-rays, gamma rays and at TeV energies both individually and in coordinated campaigns for simultaneous multiwavelength monitoring of the source. These observations indicate a complex spectral variability of the source but a clear correlation of pronounced X-ray flares with the observation of TeV photons suggests a common emission mode for the two bands.

The low energy X-ray observations of the source below 10 keV with EXOSAT, ROSAT and ASCA during the quiescent state reveal that the variability of Mkn 421 in the soft X-ray band can be interpreted as small amplitude variations about a mean luminosity level which remains almost constant (George *et al* 1988). The time scale

of these variations is of the order of 10^5–10^6 sec. The temporal analysis of the X-ray photons during the 1998 flare from the BeppoSAX data suggests that hard photons between 3 and 10 keV band lag the soft photons below 3 keV by about 10^3 sec, which is in complete contrast with the observations in the other BL Lac spectra (Fossati *et al* 2000a). The combined multi-frequency observations of the source with EUVE, ASCA, RXTE and SAX-LECS and TeV band during the 1998 active phase (Macomb *et al* 1995) indicate both positive and negative lag in individual flares (Takahashi *et al* 2000). The measured time lag is also at variance with earlier reported data (Takahashi *et al* 1996). In summary, the temporal studies in the radio and low energy X-ray band do not constrain the X-ray emission models, however, the data does show a clear correlation between the soft X-ray photons and the TeV photons. No other underlying systematic feature has emerged to date (Maraschi *et al* 1999).

The spectral measurements of the source in the X-ray band below 10 keV with BeppoSAX during 1997 and 1998 flare period show a remarkable variability and spectral evolution during the flare. The observed spectra does not appear to fit either a single power law or even a broken power law (Fossati *et al* 2000b), a curved model has been thus applied to extract the model parameters. The ν-F_ν plot in the 0.1 to 10 keV energy band however, resembles a truncated parabolic shape in all the data sets. While the description of the spectral features in a narrow 10 keV band at low energies is limited due to the inherent problems of absorption within the source region, it is likely that the source spectrum may itself consist of both thermal and non-thermal components. In the hard X-ray region above 20 keV, the available spectral data on Mkn 421 is very limited. Entire data consists of mainly pre 1990 observations from balloon-borne instruments and the recent detection of the source up to 100 keV during a flare.

In the canonical models for blazars, the observed radiation in radio, UV and low energy X-ray band, is believed to arise in the synchrotron self compton (SSC) emission from the highly relativistic electrons in the jets which are fortuitously aligned to the line of sight (Ghisellini *et al* 1985). However, in these phenomenological models the acceleration of electrons to extremely high energies of about 10^{16} eV, their survival in a strong photon field and the required energy density of these high energy electrons, still remains unresolved. Similarly, the shape of the observed spectra of BL Lac sources does not provide a definite clue for any single fundamental mechanism in the X-ray emitting region. For example, in the low energy X-ray band of 0.1–10 keV, a convex spectral shape is seen for Mkn 421, while the spectrum of ON 231 exhibits a concave profile (Tagliaferri *et al* 2000). Therefore, the hard X-ray spectra from AGNs may be composed of a superposition of multiple components arising in both thermal and non-thermal processes consisting of the synchrotron tail, synchrotron self compton contribution and possibly a compton tail produced by upgrading of the low energy photons with thermal electrons in the hot regions.

A direct way to distinguish between the thermal and non-thermal components is to observe the AGNs in the hard X-ray and soft gamma ray energy band, where the spectral breaks are expected for the thermal and Compton models. The hard X-ray spectral measurements of galactic BHC X-ray sources do show that the non-thermal spectral component which dominates the flux for energies above 30 keV does not show spectral variability and therefore, the spectral properties of the thermal component

must be inferred by computing low energy residuals. In this paper we report the spectral measurements of Mkn 421 made during the active phase in the energy band 20–200 keV. The spectral variability is studied using other available data. We also propose a continuous flaring model and list different processes which may contribute efficiently in different energy regions.

2. Instrument and observations

The observations were made with a Large Area Scintillation counter Experiment (LASE) which is designed to study fast variations in the flux of X-ray sources in the hard X-ray energy region up to 200 keV. The payload consists of three large area X-ray detector modules mounted on a servo-controlled platform. The detectors are a specially designed combination of thin and thick large area NaI(Tl) scintillation counters configured in back-to-back geometry. Each of the detector modules has a geometrical area of 400 cm^2 and the thickness of the prime detector is 4mm. The active anti-coincidence shield is provided by a 30 mm thick crystal. The field of view of each module is $4.5^\circ \times 4.5^\circ$ and is defined by a slat collimator specially designed with a sandwiched material of lead, tin and copper. Each module along with the collimator is further encased with a passive shield. Each detector is designed as a stand-alone unit with independent on-board subsystems for HV power and data processing. The payload platform is servo-stabilized and the target X-ray source and the corresponding background region are tracked using an on-board micro-processor controlled star tracker.

The back-to-back configuration of the detector gives 80% reduction in the detector background in the operating energy range, most of which is produced due to partial energy loss by the Compton scattering of high energy photons in the main detector. The pre-flight calibration of the X-ray detectors is done at different energies using radioactive sources, Cd^{109} (22.1, 87.5 keV), Am^{241} (24.7 and 59.6 keV) and Ba^{133} (32.4 and 81 keV). In addition, an Am^{241} source is mounted on the payload for the calibration of the detectors during the flight using ground command. The accepted events are pulse-height analyzed, time tagged with a 25 μ sec resolution and transmitted to ground on a 40 Kbit PCM/FM link. The details of the detector design, associated electronics, control sub-systems and in-flight behaviour of the instrument are presented elsewhere (D'Silva *et al* 1998). A 3σ sensitivity of the LASE telescope in the entire energy range up to 200 keV is $\sim 1 \times 10^{-6}$ cm^{-2} s^{-1} keV^{-1} for a source observation of 10^4 sec.

The balloon flight was launched on November 21st, 2000 from Hyderabad, India (cut-off rigidity 16.8 GV) and reached the ceiling altitude of 42 km corresponding a residual atmosphere of 2.5 mbars. A number of X-ray sources in the right ascension band of 12^h to 20^h were observed during this experiment. Mkn 421 was in the field of view of three detectors for a total period of 60 min (two sightings of 20 and 40 min each) between 0215 UT and 0350 UT and the background was measured for 20 min each before and after the source observation and for 15 min midway the source pointings. The off-source pointing location was carefully selected blank field from the known X-ray source catalog. The X-ray light curve from the all sky monitor onboard RXTE, suggests that at the time of our observation the source had transited to the active flaring phase with source luminosity twice the lowest value.

3. Results and discussion

A total excess of 6960 counts due to Mkn 421 were recorded in the three detectors in the entire energy region. This corresponds to a combined statistical significance of $\sim 7.5\sigma$. The positive excess was seen up to 200 keV. The source contribution was divided in 12 energy bins and corrected for atmospheric absorption, window transmission, detector efficiency and energy resolution for each detector and co-added. The combined spectrum of the source is shown in Fig. 1. The errors on the data points correspond to 1σ statistical errors. A systematic error of $\sim 10\%$ is estimated for the lowest energy channel and included in the plot.

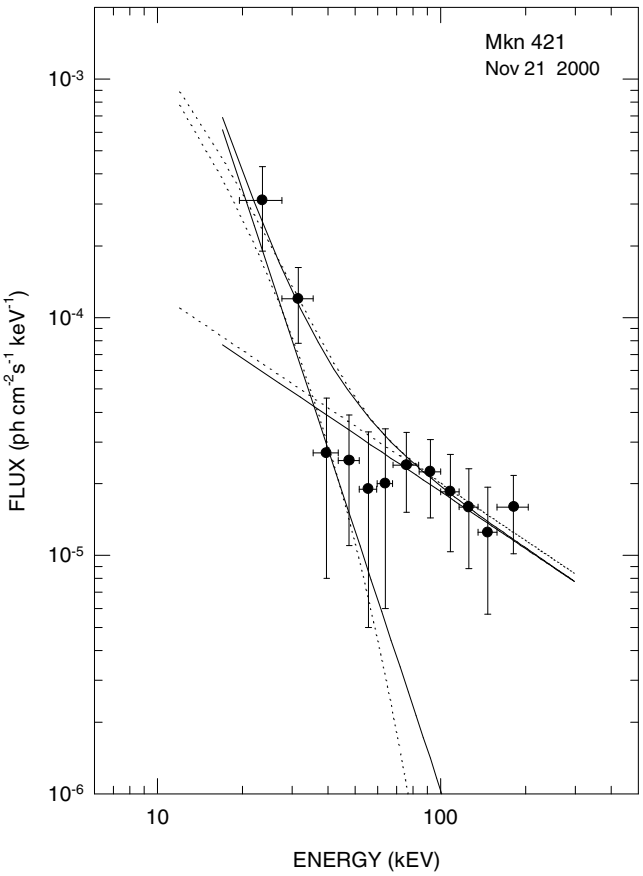

Figure 1. Hard X-ray spectrum of Mkn 421 in 20--200 keV. Solid lines represent a composite power law spectrum with two components α_1 and α_2. The dotted lines give the combination fit with α and kT.

It is clearly seen from Fig. 1, that a single power law fit of the form $\mathrm{d}N/\mathrm{d}E = K\,E^{-\alpha}$ photons $\mathrm{cm}^{-2}\mathrm{s}^{-1}\,\mathrm{keV}^{-1}$ does not fit the spectral data and the spectrum does consist of atleast two components. A broken power law or a composite fit with a thermal and non-thermal terms represent the data fairly well. The representative best fit model parameters for the two component power law model are; $\alpha_1 = -3.6 \pm 0.1$ and $\alpha_2 = -.86 \pm 0.15$ for a χ^2_4 value of 1.15 per dof. The solid line in the figure shows the power

law fit. A good fit to the data is also obtained for a composite power law + exponential function of the form $\frac{dN}{dE} = \frac{A}{E^{\alpha}} + \frac{B}{E}\, e^{-E/kT}$ ph cm^{-2} s^{-1} keV^{-1}. The best fit parameters obtained using gradient method (Bevington *et al* 1969) are $kT = 13.5 \pm 2.2$ keV and $\alpha = 0.86 \pm 0.07$ for χ^2_4 value of 1.2 per dof Lampton *et al* (1976). The estimated luminosity of the source in 20–200 band is 7×10^{42}–$10^{43} \left(\frac{D}{\mathrm{M\ pc}}\right)^2$ ergs s^{-1}.

The spectral data presented above corresponds to an active X-ray phase of the source. The long term behaviour of the source as seen in the ASM light curve on-board RXTE is shown in Fig. 2. The epoch corresponding to the present observations is marked with an arrow. A continuously varying nature of the source is quite apparent from the figure after MJD 51860, on which day the source made a transition from a lower luminosity state.

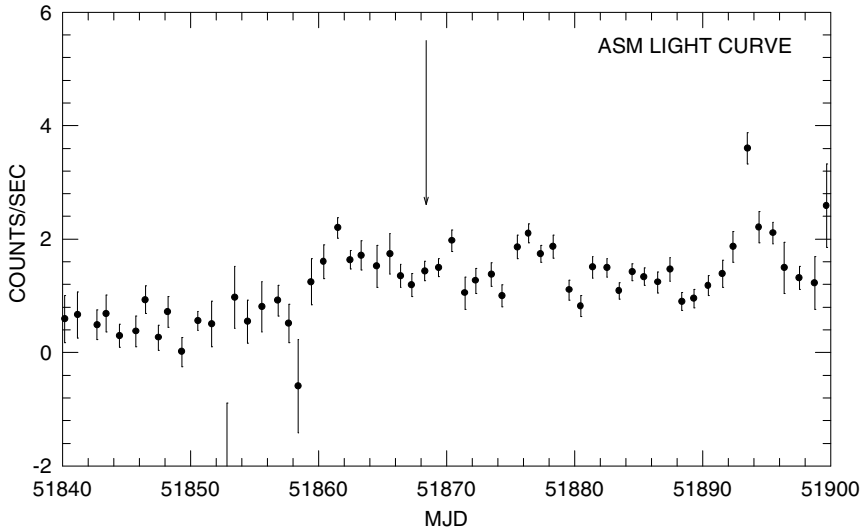

Figure 2. Long term variability of Mkn 421 in low energy range. The arrow marks the epoch for present observations.

In Fig. 3, we have plotted the available spectral measurements of the source between 1 and 200 keV band. The observations correspond to HXR 81 data (Ubertini *et al* 1984), OSO-8 data (Coe *et al* 1979) and HEAO-A2 data (Mushotzky *et al* 1979), Upper limits from OSSE observations (McNaron-Brown *et al* 1995) and the dotted line in the figure shows the single power law approximation to the BeppoSAX data (Guainazzi *et al* 1999). The hard X-ray spectral data obtained during present observations is in fair agreement with the earlier observations of Ubertini *et al* 1984, however the measured flux during the present epoch is factor of 20 higher than OSSE data in the 50–200 keV band. It is also seen from the figure that the present measurement can be construed as an extension of the OSO-8 data in the low energy band of 1–10 keV, but are in complete contrast with the HEAO-1 spectrum. Similarly, recent results of a flare spectrum in the 1–10 keV flare from BeppoSAX are also not consistent with the present measurements at higher energies. Although spectral evolution during the flare period is seen from the source in the low energy data, no simple functional form fits the data. The best fit power

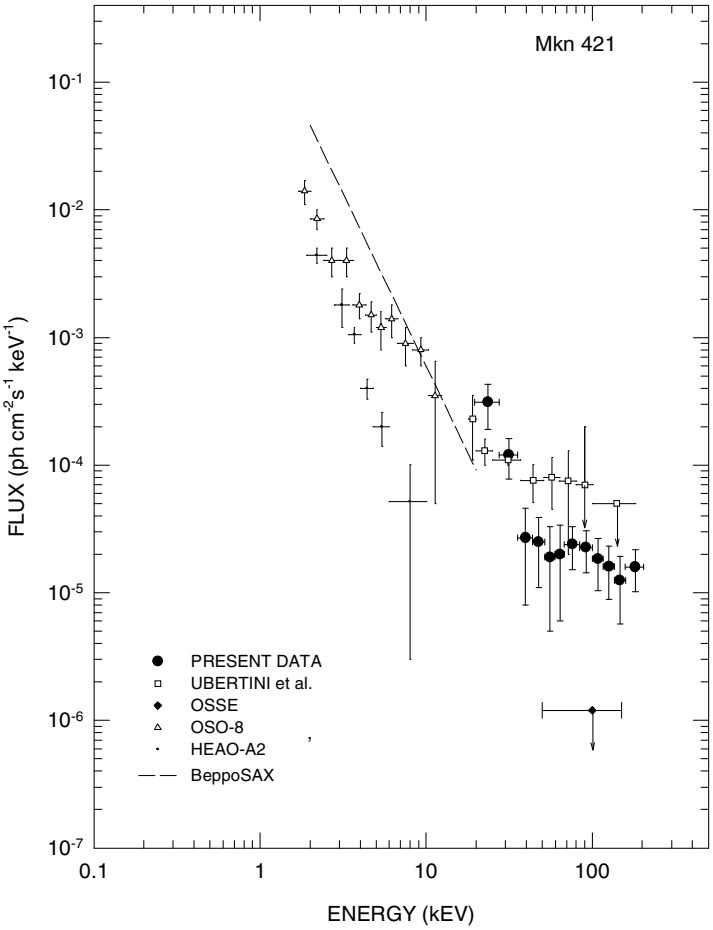

Figure 3. A comparison of the hard X-ray data of Mkn 421 with the other data in the 1.6–200 keV band.

index for a broken power law fit above 1.6 keV is $\alpha \sim 1.5$–1.8 (Fossati *et al* 2000a). It is also clear from the figure that a continuation of the low energy spectrum as shown in the dotted line, can not fit the present observations. A flattening in the spectrum above 30 keV is essential in any functional form. At the extreme high energy end, a combined fit to the hard X-ray observations and the EGRET data at GeV energies (Lin *et al* 1996) requires further steepening of the shape beyond 200 keV. In summary, a non-linear nature of the spectral shape between 1 keV and UHE energies, points to different emission mechanisms which cater to different energy regions.

4. Continuous flaring geometry

The present measurements made during the active phase clearly indicate that X-ray spectrum of the source in the 20–200 keV band is certainly not a simple power law as expected from the Synchrotron and Compton scattering models. Even if we assume that convex spectral shape in the 0.1–10 keV from BeppoSAX represents the high

energy end of the synchrotron emission, the high energy data points represent a new component. Added to this is the strong variability of the source in all wavebands. In the X-ray region, the percentage variation increases with increase in photon energies. It is therefore, necessary to examine alternate models and the possibility of thermal contribution to the X-ray spectrum. A new look is also necessitated, for the particle acceleration to higher energies. It is also essential that TeV photons must originate in a region where the magnetic field is extremely low, in order to avoid strong attenuation of these photons through magnetic pair-production process. An approximate limit is given by $\sqrt{B^2}[G] < 10^{12} \times \epsilon / E_{ph}$ (Bednareck 1991).

We therefore, propose a continuously flaring model in which the particle flux consisting of protons and electrons is squirted during each flaring episode and which is accelerated in the relativistic jets. Random nature of the intensity variations of Mkn 421 in different wavelength bands supports such a geometry. A steady emission from the source points to continuous injection of the particles into the jets.The active phase is therefore, analogous to the increase in the amplitude and the flare occurrence rate. Considering that the large flares are the high amplitude sub-set of continuum of low level flares and lead to a variability of the ambient particle flux, one can account for the observed temporal behaviour of the source even at ultra high energies.

4.1 *Particle acceleration and the photon emission*

The photon spectrum of Mkn 421 extends from radio emission to TeV ($> 10^{12}$ eV) gamma ray energies and is highly variable. The observation of a jet in the source provides a natural basis for radio emission as due to synchrotron emission from high energy electrons. The formation of the jet features, their morphology, extent and the speed of expansion are ultimately ascribable to either the accretion on to the central black hole or episodic ejection from the centre of the galaxy. The dynamical parameters including mass flow, momentum, collimation, energy, magnetic flux and the cooling depend upon the ambient environment and many hydro-dynamical models of the formation of narrow jets for AGN's and stellar scale compact objects have been proposed in literature (Begelman *et al* 1984, Colgate 1990). A continuous input to the jets as envisaged above does require the formation of accretion disk and the transfer of the material to the base of the jet. For synchrotron emission from relativistic electrons, the electron energy corresponding to the observed radio emission lie in the range $E \simeq 300 - 2000 \times [\nu / H_{\perp}]^{1/2}$ eV. Hence the detection of radio flux from the source is itself an evidence of the presence of relativistic particles and *in situ* acceleration.

The particle acceleration in the jets is believed to be due to shock wave at the interaction boundary of the expanding relativistic plasma and the ambient environment. During the shock acceleration a particle with velocity v gains a momentum $\simeq w/v$ every time it crosses the shock of velocity w. If the particles are scattered efficiently both sides of the shock and stay trapped, the particle can reach relativistic energies provided the adiabatic losses are negligible. In case of the diffusive shock the maximum proton energy $E^{p}_{\max} \sim 10^{15}$ eV is attainable for a shock compression ratio of 4 and reasonable values for other parameters (Ogelman 1986). Treating ultrasonic turbulent mass flow in the jet stream as analogous to the strong stellar winds the maximum energy may be even higher by ~ 100 at the shock boundary (Cesarsky & Montmerle 1991). In shock acceleration, the resultant spectrum of the particles is a power law and for a shock compression of $\sim 3 - 4$ the exponent lies between 2 and 2.5.

A large population of high energy electrons within a strong radio photon field can also give rise to high energy X-ray photons due to Inverse Compton collisions. This SSC mechanism is generally believed to be the main operative process for photon emission in the AGN sources. The SSC mechanism however, predicts very definite relationship between the spectral indices in the radio and the X-ray energy bands with the electron spectrum. If we take the spectral index for the electron spectrum to be $\gamma \sim 2.5$, then the power index for the synchrotron photon flux is given by $\alpha = \frac{(\gamma-1)}{2} - 1 \sim -1.75$. With the estimated value of $B \sim 0.03\,\mathrm{G}$, a break in the incident electron spectrum and a change of the power index by ≥ 1, due to steepening caused by the synchrotron and bremsstrahlung losses is expected at electron energies above 10^{14} eV. One can therefore, infer a further steepening in the photon spectrum by ≥ 0.5 at higher energies. Furthermore, the energetic constraints provide that the flux of X-ray photons produced in Compton collision of high energy electrons with radio photons increases, if value of B decreases, which in turn requires much higher electron energy for the production of radio photons. The observed X-ray spectrum below 20 keV can therefore, be identified with the tail end of the SSC photons. A flattening in the X-ray spectrum in hard X-ray region and a change of spectral index from 3.6 to 0.86 can not be therefore, ascribed to a non-thermal origin. As seen in Fig. 1. an additional component dominating the hard X-ray flux above 60 keV is essential. We propose that the high energy component arises due to upgrading low energy photons by thermal electrons.

It is well known that a localized non-radiative heating of the plasma can take place near the shock front. Therefore, a significant fraction of soft X-rays in the 2–10 keV region may arise due to thermal bremsstrahlung emission at the collision boundary of the jet since temperature of the hot gas behind the shock is $\sim 10^7 - 10^8\,\mathrm{K}$. The presence of an iron line at 6 keV in the spectrum clearly points to the existence of high temperature regions of thermal emission within the source volume. In addition, the observations of soft excess in bright quasars, without any obvious correlation with other spectral properties of the source is also indicative of a thermal component in the quasars spectra. Upgrading of the low energy seed photons due to multiple Compton collision with thermal electrons can lead to Compton tail in the 40–200 keV energy range as seen in the Mkn 421 spectrum. During Comptonization, if $4\,\mathrm{kT}_e > h\nu$, the seed photons will be upgraded in energy. The increase in photon energy on average during each scattering is given by $\Delta\epsilon = \frac{4}{3}[\gamma^2 - 1]\epsilon$, even for a Maxwellian distribution of electrons with $\mathrm{kT}_e \ll m_e c^2$. Therefore, multiple scattering even by a Maxwellian gas in hot spots can lead to very high photon energies. The emergent spectrum is a unified power law but the exact spectral shape is radically modified if the seed photons have a spectral distribution and there is a temperature gradient in the scattering electron cloud.

Since the correlated measurements have revealed beyond doubt that TeV gamma rays have a one-to-one correspondence with the low energy X-ray emission from the source, one is tempted to assume the TeV emission to be a simple extension of the SSC spectrum. However, an enhancement by a factor of 10^9 in the energy of electrons is needed to emit TeV photons and is far more difficult to achieve due to long acceleration time scale given by $t_a \sim (c/v)^2 t_c$, where t_c is the collision time, which is necessary to reach these energies, against the efficient cooling due to synchrotron and bremsstrahlung processes. Recently Dermer and Schlickeiser (1991) have shown that

production of UHE gamma rays by the inverse Compton process is not plausible even if one considers the 'triplet pair production' process. A much more efficient way of producing TeV gamma rays is from the protons. UHE photons can arise from the π° decay which are produced due to the collisions of the accelerated proton component. The production of gamma ray per target nuclei in pp collisions is given by Ozel & Ficktel (1988); $q[E_\gamma]\ \mathrm{d}E_\gamma = \mathrm{d}E_\gamma \int R(E_\gamma, E_p) N_p(E_p)\ \mathrm{d}E_p$; where R represents the integrated gamma ray production rate based upon the π° meson production and distribution function and N_p is the proton number density. The integral gamma ray flux from the source volume can be written as $S_\gamma \sim 2 \times 10^{25} \eta n_H V$, where V is the volume of the source, n_H is the number density of hydrogen nuclei and η is the ratio of the proton spectral density to that in the vicinity of the earth. Another possible source for the emission of TeV photons is due to $p\gamma$-photomeson photo production process. The gamma ray yield efficiency in this case is higher by a factor of ~ 2 since the square mass invariant in pp collisions is higher than the corresponding $p\gamma$ collision with X-ray photons. The estimated efficiency in the first process is only $\sim 8\%$. In addition, the multiplicity of pions in pp collisions increases with energy and this results in lower energy gamma ray photon for a given proton energy compared to $p\gamma$ process. The observable flux from the jet region will correspond to an oriented directional beam with a solid angle Ω. The required proton luminosity for a detectable gamma ray flux of $\sim 10^{-8}$ ph cm^{-2} s^{-1} keV^{-1} in the gamma ray region will require a number density of emitting protons given by $L_p \sim 3 \times 10^{44} \times \Omega \times \left(\frac{D}{\mathrm{Mpc}}\right)^2$. An apparent simultaneity of the TeV and X-ray photons is maintained in the proposed process as both the electron and protons are accelerated at the same time. This may also explain the observed feature that the decay of the TeV flux is faster than the keV flux.

In conclusion, the presence of jet in Mkn 421 does provide a self consistent basis for the acceleration of the electrons and protons within the source volume. The emission of ultra high energy photons can easily be produced in *pp* collisions. The observation of two component power-law X-ray spectrum of the source, with clear flattening at higher energies does not support a pure Synchrotron Self Compton emission model or the continually curved model proposed by Malizia *et al* (2000). The data points to an additional component possibly arising from thermal Comptonization in the hot regions within the emission volume.

Acknowledgements

I wish to thank the dedicated support of J. A. R. D'Silva, P. P. Madhwani, N. V. Bhagat, B. G. Bagade and Ms. N. Kamble. The BATSE and RXTE teams are gratefully acknowledged for their archival data.

References

Bednarek, W. 1991, 22nd ICRC Dublin, **1**, 549.
Begelman, M. C., Blandford, R. G. Rees, M. J. 1984, *Rev. Mod. Phys.*, **56**(2), 255.
Bevington, P. R. 1969, *Data reduction and Error analysis* (McGraw Hill).
Cesarsky, C. J., Montmerle, T. 1991, *Sp. Sci. Rev.* **36**, 173.
Coe, M. S., Dennis, B. R., Dolan, J. F. *et al* 1979, *Ap. Letters*, **20**, 63.

Colgate, S. A. *et al* 1990, *Astro. Lett. and Commun.*, **27**, 411.
Dermer, C. D., Schlickeiser, R. 1991, *Astron. Astrophys.*, **252**, 414.
D'Silva, J. A. R., Madhwani, P. P., Tembhurne, N. T., Manchanda, R. K. 1998, *NIM*, **A421**, 342.
Fossati, G., Celotti, A., Chiaberge, M. 2000a, *Astrophys. J.*, **541**, 153.
Fossati, G., Celotti, A., Chiaberge, M. 2000b, *Astrophys. J.*, **541**, 166.
George, I. M., Warwick, R. S. and McHardy, I. M. 1988, *MNRAS*, **235**, 787.
Ghisellini, G., Marascii, L., Treves, A. 1985, *Astr. Astrophys.*, **146**, 204.
Guainazzi, M., Vacanti, G., Malizia, *et al* 2000, *Astron. Astrophys.*, **342**, 124.
Lampton, M., Morgan, B., Boyer, S. 1976, *Astrophys. J.*, **208**, 177.
Lin, Y. C., Bertsch, D. L., Dingus, B. L. *et al* 1996, *Astr. Astrophys.*, **120**, 449.
Macomb, D. J., Akerlof, C. W., Aller, D, 1995, *Astrophys. J.* **449**, 99.
Malizia, A. *et al* 2000, *MNRAS*, **312**, 123.
Maraschi, L., Fossati, G. and Tavecchio F. 1999, *Astrparticle Phys.*, **11**, 189.
McNaron-Brown K., Johnson W. N., Jung, G. V. *et al* 1995, *Astrophys. J.* 575.
Mushotzky, R. F., Boldt, E. A., Holt, S. S., Serlimitsos, P. J. 1979, *Astrophys. J. (Letters)*, **232**, L17.
Ricketts, M. J., Cooke, B. A., Pounds, K. A. 1976, *Nature*, **259**, 546.
Tagliaferri, G., Ghisellini, G., Giommi, P. *et al.* 2000, *Astr. Astrophys.*, **354**, 431.
Takahashi, T. *et al.* 1996, *Astrophys. J.*, **470**, L 89.
Takahashi, T., Katoka, J., Madejski, G. *et al.* 2000, *Astrophys. J. (Letters)*, **542,** L105.
Ubertini, P., Bazzano, A., LaPadula, C., Polcaro, V., Manchanda, R. K. 1984, *Astrophys. J.*, **284**, 54.
Ogelman, H. 1986, in *Int. School of NS, AGN and Jets*, Erice.
Ozel M, Fichtel, C 1988, *Astrophys. J.*, **335**, 135.